American Mineralogist, Volume 91, pages 560–567, 2006

The high-pressure phase transformation and breakdown of $MgFe_2O_4$

SOFIA WINELL,[1,*] HANS ANNERSTEN,[1] AND VITALI PRAKAPENKA[2]

[1]Department of Earth Sciences, Uppsala University, SE 752 36 Uppsala, Sweden
[2]Consortium for Advanced Radiation Source (CARS), University of Chicago, Chicago, Illinois 60637, U.S.A.

ABSTRACT

The high-pressure transformation of $MgFe_2O_4$ was studied by Mössbauer and Raman spectroscopy and synchrotron X-ray diffraction using the DAC technique and laser annealing at temperatures of 1500–2000 K. The high-pressure phase of $MgFe_2O_4$ was observed from in situ Mössbauer spectra at 17 ± 1 GPa after laser annealing by the appearance of two quadrupole doublets. This indicates a disordered distribution of Mg and Fe in an early stage. The displacive nature of the transformation of the spinel into its high-pressure polymorph was shown at increasing pressure by the redistribution of iron into only one site. After decompression Mössbauer spectroscopy revealed the presence of Fe_2O_3 in the sample. This was further confirmed by Raman spectroscopy at ambient conditions and by in situ high-pressure XRD, indicating a partial breakdown of the spinel into its constituent oxides MgO and Fe_2O_3. The XRD pattern of the high-pressure phase of $MgFe_2O_4$ can be indexed in agreement with the $CaMn_2O_4$-type structure, with cell parameters $a = 2.775(2)$, $b = 9.283(16)$, and $c = 9.446(5)$ Å at 23 ± 2 GPa. The multiphase spectra from all three analytical methods suggests that inhomogeneous conditions prevailed in the DAC experiments, resulting in two different reactions at high pressure and temperature, i.e., $T < 1800$ K: $MgFe_2O_4 \rightarrow Fe_2O_3 + MgO$ and $T > 1800$ K: $MgFe_2O_4 \rightarrow$ hp-$MgFe_2O_4$.

Keywords: High-pressure studies, magnesioferrite, phase transition, Mössbauer spectroscopy, XRD data

INTRODUCTION

Because spinels are important minerals in the Earth mantle rocks, their properties have been the subject of many studies. At increasing pressure and temperature they either transform into a high-pressure phase or break down into constituent oxides (Ringwood and Reid 1969). Thermodynamics for magnesioferrite, $MgFe_2O_4$, predicts the breakdown of its structure into periclase, MgO, and hematite, Fe_2O_3, at elevated pressure and temperature. Since iron and magnesium are two of the most important constituents of the mantle, the study of the high-pressure behavior of $MgFe_2O_4$ may provide information useful in understanding the Earth's interior. In addition, host phases for the possible existence of Fe^{3+} in the mantle are not fully clarified and $MgFe_2O_4$ may be one of the candidates.

Magnesioferrite is an inverse ferrimagnetic spinel at ambient temperature and pressure that crystallizes in the cubic space group $Fd3m$ ($Z = 8$). To describe the inverse structure magnesioferrite may be written as $(Mg_{1-x}Fe_x)(Mg_xFe_{2-x})O_4$, where x is the temperature-dependent inversion parameter.

Thermodynamic calculations of many AB_2O_4 spinels show that at high pressure the spinel structure becomes unstable with respect to its constituent oxides, resulting in breakdown of that structure. However, as shown experimentally, this is not always the case; instead, many spinels transform directly into a denser post-spinel phase. Ringwood and Reid (1969) experimentally investigated the high-pressure transformation of several spinels. They observed transformations which earlier had only been predicted from thermodynamic calculations. The suggested structure types for the dense post-spinel phase are $CaFe_2O_4$, $CaMn_2O_4$, and $CaTi_2O_4$, where the large Ca^{2+} ion is eight-coordinated and the smaller M^{3+} ($M^{3+} = Fe^{3+}$, Mn^{3+}, Ti^{3+}) ions are six-coordinated with oxygen. The three high-pressure structures differ in the degree of distortion.

Several experimental studies confirmed the results of Ringwood and Reid (1969). Liu (1975) observed the breakdown of spinel, $MgAl_2O_4$, into the constituent oxides MgO and Al_2O_3 at a pressure above 15 GPa and a temperature between 1000-1400 °C. Irifune et al. (1991) reported the formation of a high-pressure phase of $MgAl_2O_4$ from the breakdown products above 25 GPa and 1500 °C, with the $CaFe_2O_4$-type structure. Further studies by Funamori et al. (1998) revealed that this $CaFe_2O_4$-type structure of $MgAl_2O_4$ transforms to the $CaTi_2O_4$-type structure above 40 GPa, using laser heating at temperatures between 2000 and 3000 K.

Due to its postulated presence in the mantle, magnetite (Fe_3O_4) is one of the most investigated spinels under high pressure. Extensive solid solution exists between $MgFe_2O_4$ and Fe_3O_4. Both have the inverse spinel structure and contain Fe^{3+}, which is of special interest because of the unclear role of Fe^{3+} in the lower mantle. The high-pressure phases of Fe_3O_4 and $MgFe_2O_4$ were first observed by Mao et al. (1974) and Mao and Bell (1974), respectively, using in situ X-ray diffraction at pressures above 20 GPa. The formation of high-pressure phases of Fe_3O_4 and $MgFe_2O_4$ was further confirmed from Mössbauer spectroscopy by Mao et al. (1977), appearing as non-magnetic phases at room temperature. In a second Mössbauer study of Fe_3O_4 up to 66 GPa at 300 K by Pasternak et al. (1994), two distinct iron sites belonging to the high-pressure phase could be seen in the Mössbauer spectra. Based on synchrotron XRD, Fei et al. (1999) suggested

* E-mail: sofia.winell@geo.uu.se

that the high-pressure phase of Fe_3O_4 is of the $CaMn_2O_4$-type. However, Haavik et al. (2000) proposed the $CaTi_2O_4$-type. The latter suggestion has recently been supported by Dubrovinsky et al. (2003) and Lazor et al. (2004). Huang and Bassett (1986) demonstrated the pressure-temperature dependence of the phase transformation. According to thermodynamic calculations, Fe_3O_4 should break down to FeO and Fe_2O_3 at 13.3 GPa at ambient temperature and then transform to the high-pressure phase at around 35 GPa (Lazor et al. 2004, Fig. 3). $MgFe_2O_4$ is also expected to break down at increasing pressure, but prior to the present investigation this had not been experimentally confirmed. Andrault and Bolfan-Casanova (2001) performed a high-pressure in situ X-ray diffraction investigation of $MgFe_2O_4$ using laser annealing. The first sign of the phase transformation was observed at 20.2 GPa after the first laser annealing and a mixture of the low-and high-pressure phases could be seen up to 27.2 GPa. Their Rietveld structure refinements of the high-pressure phase perfectly match the $CaMn_2O_4$-type structure. A Raman spectroscopy study of $MgFe_2O_4$ performed at room temperature and high pressure by Wang et al. (2002) revealed no indications of breakdown, but a direct transformation to the high-pressure phase at 27.7 GPa. Levy et al. (2004) determined the equation of state of $MgFe_2O_4$ and modeled its phase relations from elastic and thermal properties measured in separate high-pressure and high-temperature experiments. Their phase diagram suggests a stability field of coexisting MgO and Fe_2O_3 at $T < 1800$ K that expands with increasing pressure and decreasing temperature (Fig. 1). At $T > 1800$ K, $MgFe_2O_4$ directly transforms into the orthorhombic high-pressure phase when the pressure is increased. A maximum pressure of around 17 GPa was estimated for the stable oxide mixture at ~1800 K. Levy et al. (2004) did not observe any sign of transformation at pressures up to 35 GPa in their experiments.

The aim of the present study was to further clarify the behavior of $MgFe_2O_4$ at high pressure and temperature. Using the diamond anvil cell (DAC) technique we employed in situ high-pressure Mössbauer spectroscopy and synchrotron X-ray diffraction and, at ambient conditions, Raman spectroscopy. Laser heating was applied at high pressure and at temperatures between 1500-2000 K, the relevant range to study the phase relations of $MgFe_2O_4$ at the studied pressures. Special emphasis was put on the breakdown reaction of $MgFe_2O_4$ into its constituent oxides, as well as on the nature of the direct transformation to a denser post-spinel phase.

Experimental methods

Sample synthesis

The synthesis of $MgFe_2O_4$ was performed according to O'Neill et al. (1992), with some MgO in excess and with Fe_2O_3 36% enriched in ^{57}Fe. To determine the lattice parameter of the synthesized $MgFe_2O_4$, a portion of the sample was mixed with an Si standard and measured using a Siemens D5000 diffractometer with Cu$K\alpha_1$ = 1.540598 Å. The diffraction pattern was collected from 27 to 149° 2θ and the lattice parameter, a_0, was then refined by a least-squares refinement using the program Unitcell, giving $a_0 = 8.3828(2)$ Å. This corresponds to an inversion parameter, x, of 0.88 (O'Neill et al. 1992). No additional phases were detected. Further characterization of $MgFe_2O_4$ was made from well-resolved Mössbauer spectra obtained in an external magnetic field separating the tetrahedral and octahedral ferric iron ions. Intensities of the two distinct absorption patterns indicated an inversion parameter of $x = 0.85(1)$.

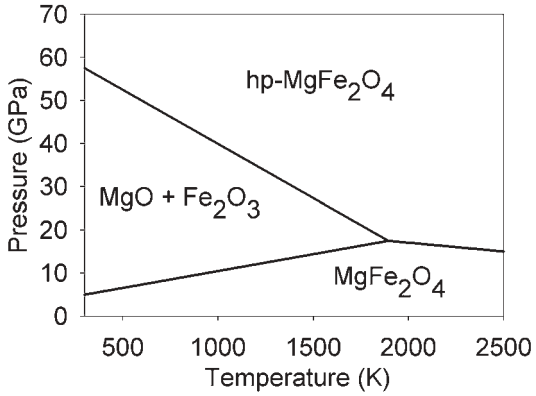

Figure 1. Phase relations of $MgFe_2O_4$ schematically redrawn from Levy et al. (2004).

Mössbauer spectroscopy

A ^{57}CoRh point source was used for the Mössbauer measurements at room temperature. The velocity calibration was made against metallic iron.

Experiments were conducted in two different DAC's, both with a 200 µm gasket hole drilled in preindented Re-foil. $MgFe_2O_4$ was loaded in the sample hole together with CsCl as a hydrostatic pressure medium and chips of ruby as an internal pressure calibrant. To promote reaction, the first sample was heated three times and the second four times using an Nd:YAG laser with a heating spot diameter of ≈20 µm, which was scanned over the sample. The temperature was in the range 1500–2000 K and no melting of the samples was observed. In situ room-temperature Mössbauer spectra at different pressures were each measured for 2–5 days in transmission mode. The mirror symmetric spectra (512 channels) were folded and computer-fitted using a program developed by Jernberg and Sundqvist (1983).

Raman spectroscopy

The diamond anvils failed in one of the DACs used in the Mössbauer experiments. This sample, originally loaded with CsCl as the pressure medium, was demounted from the DAC and studied with Raman spectroscopy at ambient conditions. The Raman system consisted of an imaging spectrometer (HoloSpec, Kaiser) equipped with a thermoelectrically cooled CCD detector (Andor). Raman emission was exited in the back-scattering geometry by the 514.5 nm line of an Argon ion laser providing up to 50 mW of power. Two holographic super notch filters (Kaiser) were used to reject the Rayleigh line. Fourteen spectra were collected from different parts of the sample with an acquisition time of 15–30 min.

Synchrotron X-ray diffraction

The high-pressure X-ray diffraction data were collected at the APS, Argonne National Laboratory synchrotron radiation facility, beam line HP-CAT sector 16. A DAC with a 150 µm hole drilled in a pre-indented Re gasket was loaded with $MgFe_2O_4$ sample, with Al_2O_3 as the pressure medium and ruby chips for pressure determination. In situ high pressure and room temperature XRD spectra were obtained after two periods of laser heating at 1500–2000 K. Pressure, measured from the ruby directly after the last period of annealing, was 25 ± 3 GPa. The pressure calculated from the P-V EOS for Al_2O_3 given by d'Amour et al. (1978) using three to five diffraction lines, (102), (104), (113), (024), and (300), was between 21 and 25 GPa in the 11 different spots. The angle-dispersive synchrotron X-ray diffraction experiments were performed using a wavelength of 0.4228 Å and a beam diameter of ~15 µm. Diffraction data were integrated from the two-dimensional images into one-dimensional diffraction patterns using the program Fit2d (Hammersley et al. 1996). The peaks were fitted by Voigt amplitude profiles using the program PeakFit.

Results

Mössbauer spectroscopy

Mössbauer spectra of $MgFe_2O_4$ in DAC 1 under zero pressure show two closely overlapping magnetically split patterns

from Fe^{3+} in the spinel structure: sites 1 and 2 in Figure 2a. The hyperfine parameters at ambient temperature and pressure, presented in Table 1, show typical values for ferric iron at the octahedral and tetrahedral sites (O'Neill et al. 1992). A stepwise increase in pressure was applied and spectra were concurrently collected at eight additional pressures. At around 21 GPa the high-pressure phase of $MgFe_2O_4$ was observed and after the first laser annealing (when the pressure dropped to 17 ± 1 GPa) it was clearly seen as two paramagnetic doublets in the middle of the Mössbauer spectrum: sites 3 and 4 in Figure 2b. The intensity ratio for the two iron-containing high-pressure sites was at this stage similar to that in the spinel phase. As the pressure increased, more $MgFe_2O_4$ transformed into the high-pressure phase and a change in intensities and hyperfine parameters for the two doublets was observed. Figure 3 shows how the isomer shift (IS) and quadrupole splitting (QS) changed with increasing pressure for the high-pressure phase, sites 3 and 4, in DAC 1. However, due to a large pressure gradient in the sample chamber at increasing pressure, an average of the measured pressures is given in Figure 3. The two final measurements have a pressure gradient of ± 8 GPa. Despite this large pressure gradient, a clear trend was observed for the two high-pressure sites. At 17 ± 1 GPa, site 3 has a low isomer shift (IS = 0.21 mm/s) and a large quadrupole splitting (QS = 2.47 mm/s), but as pressure increased, the IS increased and the QS decreased for this site (Fig. 3). Simultaneously, the intensity decreased for site 3 and increased for the pattern of site 4. The hyperfine parameters for site 4 did not change significantly throughout the experiments, as is shown in Figure 3.

Due to the large pressure gradient and a low counting rate in the Mössbauer spectrometer, an additional DAC was prepared (DAC 2) when a new point source was installed. The $MgFe_2O_4$ sample was from the same batch as in DAC 1. In this second DAC experiment, the pressure was directly increased to 24 ± 4 GPa before the first laser annealing. A further increase in pressure to 29 ± 4 GPa was followed by three additional periods of laser annealing. A spectrum obtained at 29 ± 4 GPa, Figure 2c, shows the two doublets from the high-pressure phase, similar to the DAC 1 experiment. The IS for sites 3 and 4 (0.46 and 0.31 mm/s, respectively) and the QS (1.61 and 0.60 mm/s, respectively) are, however, both lower than at the corresponding pressure in the first DAC experiment. Additionally, the magnetically split patterns have narrower line width and larger hyperfine fields as compared to the DAC 1 experiment.

In an effort to further increase pressure in DAC 2 the diamond anvils failed and a Mössbauer spectrum was collected from the

TABLE 1. Mössbauer hyperfine parameters for the spectra in Figure 2

			IS (mm/s)	QS (mm/s)	B (Tesla)	I (%)	*P* (GPa)
DAC 1	a	1	0.32	0.03	48.2	57	0
		2	0.28	–0.02	44.9	43	
	b	1	0.30	0.07	49.1	39.5	17 ± 1
		2	0.26	0.00	46.6	33.2	
		3	0.21	2.47	–	12.0	
		4	0.44	0.49	–	15.3	
DAC 2	c	1	0.31	0.41	51.1	14.7	29 ± 4
		2	0.29	0.14	49.4	29.7	
		3	0.46	1.61	-	17.4	
		4	0.31	0.60	-	38.3	
	d	1	0.38	–0.174	51.3	16.1	0
		2	0.38	–0.242	45.7	28.1	
		3	0.90	1.35	–	4.7	
		4	0.33	0.85	–	51.2	

Note: The letters (a, b, c, d) and the numbers (1, 2, 3, 4) refer to the letters and numbers in Figure 2.

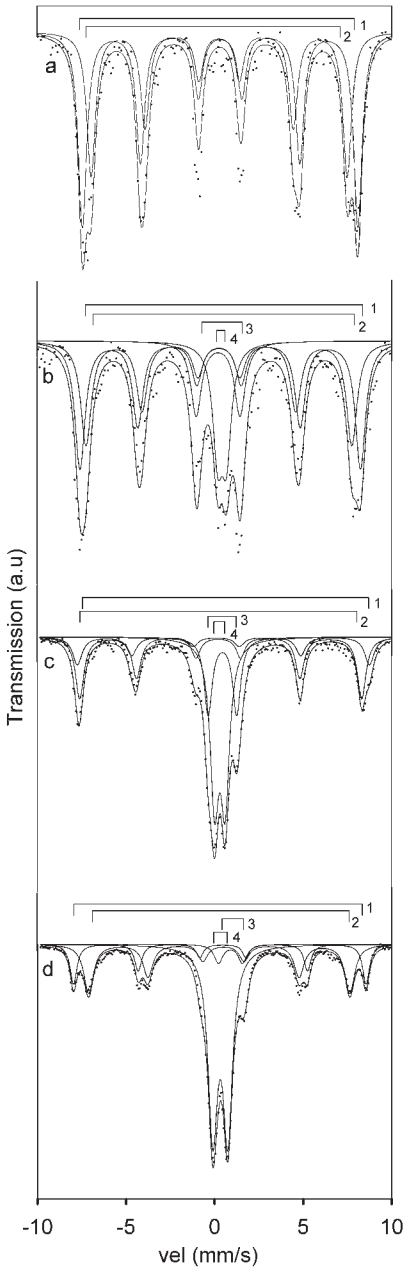

FIGURE 2. (**a**) Mössbauer spectra of $MgFe_2O_4$ at ambient conditions in DAC 1. 1 = octahedral site, 2 = tetrahedral site. (**b**) Mössbauer spectra of $MgFe_2O_4$ and the high-pressure phase at 17 ± 1 GPa in DAC 1. 1 = octahedral site in $MgFe_2O_4$, 2 = tetrahedral site in $MgFe_2O_4$, 3 and 4 = high-pressure sites. (**c**) $MgFe_2O_4$ and the high-pressure phase at 29 ± 4 GPa in DAC 2. 1 = Fe_2O_3, 2 = $MgFe_2O_4$, 3 and 4 = high-pressure sites (**d**) Mössbauer spectra of the decompressed sample in DAC 2. 1 = Fe_2O_3, 2 = $MgFe_2O_4$, 3 = $(Fe^{2+}, Mg)O$ or alternatively the dodecahedral site in the high-pressure phase, 4 = octahedral site in the high-pressure phase.

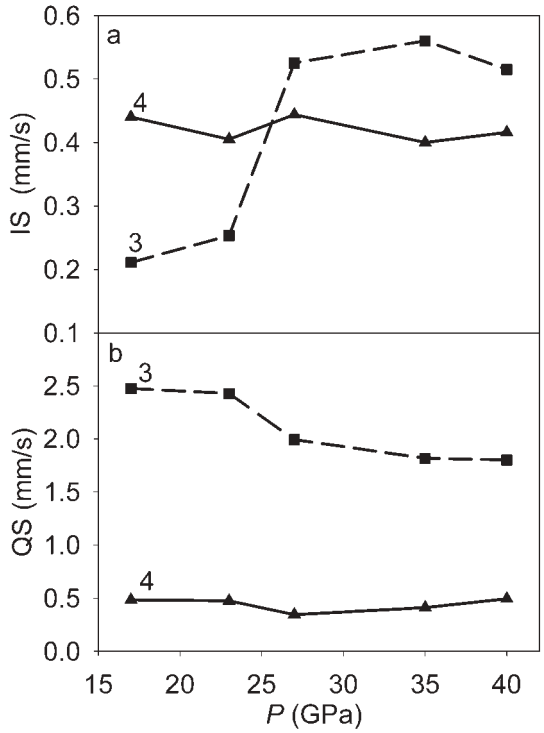

FIGURE 3. Diagram showing (**a**) IS and (**b**) QS vs. pressure for the high-pressure phase in DAC 1. The markers (▲, ■) are placed at the average pressure in the DAC at which the different measurements were done.

decompressed sample. This spectrum is shown in Figure 2d. One intense doublet now dominates the spectrum, site 4, but one small additional doublet is also present. Due to the low intensity of this second doublet it is difficult to obtain a reliable fit to the pattern. Depending on fitting procedure, the IS varies between 0.63 and 0.90 mm/s and the QS between 1.92 and 1.35 mm/s. The χ^2 value is slightly lower for the fit with the higher IS and lower QS, which is the one shown in Figure 2d. The doublet could indicate a remnant site 3, or formation of an $(Mg,Fe^{2+})O$ solid-solution. Additionally, there are two well-resolved magnetically split sextets in the decompressed spectrum. The value of the hyperfine field of the outer sextet, site 1 in Figure 2d, is 51.3 T, which is too high to represent $MgFe_2O_4$. Instead we assigned this sextet to α-Fe_2O_3 (Greenwood and Gibb 1971). The pattern with the smaller hyperfine field would then correspond to the closely overlapping sextets of the remaining low-pressure spinel. The sextet with the magnetic field 51.1 T, site 1 in Figure 2c, is most likely also dominated by Fe_2O_3.

The observed Fe_2O_3 and the possible presence of $(Mg,Fe^{2+})O$ demonstrates a partial breakdown of the $MgFe_2O_4$ sample into the constituent oxides MgO and Fe_2O_3.

Raman spectroscopy

To further confirm the breakdown of $MgFe_2O_4$ into its constituent oxides, MgO and Fe_2O_3, as detected in the Mössbauer experiment, we applied Raman spectroscopy at ambient conditions on the decompressed sample after failure of the diamond anvils. Assuming a partial breakdown of $MgFe_2O_4$, based on the Mössbauer data, three Raman active phases should appear, i.e., $MgFe_2O_4$, Fe_2O_3, and the high-pressure phase of $MgFe_2O_4$. CsCl, used as the pressure medium in the initial high-pressure Mössbauer experiment, is not Raman active. In the investigation by Wang et al. (2002) five Raman active modes for $MgFe_2O_4$ were observed at ambient conditions ($A_{1g} + E_g + 3F_{2g}$). For Fe_2O_3 there are seven well-known Raman modes ($2A_{1g} + 5E_g$) below 700 cm^{-1} and a two-phonon mode at 1320 cm^{-1} (McCarty 1988; Massey et al. 1990; Shim and Duffy 2002). Additionally, a weak two-magnon mode at ~1540 cm^{-1} was calculated and experimentally observed by Massey et al. (1990). Concerning the high-pressure phase, three Raman modes ($B_{(1-3)g} + 2B_{(1-3)g}$) remain stable after decompression according to Wang et al. (2002). However, these peaks are very weak and are not expected to be distinguished in the presence of the other two phases, Fe_2O_3 and $MgFe_2O_4$.

In six of the 14 collected spectra, traces of Fe_2O_3 are evident. Figure 4a is a spectrum mainly consisting of $MgFe_2O_4$ and Figure 4b a spectrum consisting both of $MgFe_2O_4$ and Fe_2O_3. For comparison, a spectrum of pure Fe_2O_3 is shown in Figure 4c. Considering the history of the sample, including compression to 29 ± 4 GPa, laser annealing, and fast decompression (when the diamond anvils failed) the $MgFe_2O_4$ spectrum in Figure 4a is in good agreement with the spectra presented by Wang et al. (2002). Overlap between $MgFe_2O_4$ and Fe_2O_3 limits the number of peaks to the one at ~400 cm^{-1}, which indisputably comes from Fe_2O_3 (Fig. 4b). However, compared to the spectrum dominated by $MgFe_2O_4$ in Figure 4a, additional peaks in the 200 and the 300 cm^{-1} regions also indicate the presence of the Fe_2O_3 phase. Additionally, Fe_2O_3 has two peaks at ~1320 and ~1540 cm^{-1}; we suggest that the major contribution to the two peaks in this area in our spectra comes from Fe_2O_3. However, our spectra, especially the one in Figure 4d, show similarities with those in Prakapenka et al. (2003/2004). In that micro-Raman study the formation of carbon phases (usually microcrystalline graphite) in DAC experiments was demonstrated. We therefore suggest a possible contribution from carbon phases to the two peaks at wave numbers > 1300 cm^{-1}. Still, the intensity ratio for these two peaks in our spectra is reversed compared to those in Prakapenka et al. (2003/2004), and therefore further supports the suggestion that the main contribution to these peaks arises from Fe_2O_3 rather than carbon phases.

Synchrotron X-ray diffraction

A total of 11 spots were analyzed in the sample at room temperature after two periods of laser heating and at an average pressure of 23 ± 2 GPa. The heating temperature was 1500–2000 K, which is the relevant range to study the phase relations of $MgFe_2O_4$ at this pressure (Fig. 1). The pressure was calculated from the peak positions of Al_2O_3.

The results can be divided into three major categories: spots with almost complete transformation of $MgFe_2O_4$ into its high-pressure form (Fig. 5a), predominantly disproportion of $MgFe_2O_4$ into its constituent oxides MgO and Fe_2O_3 (Fig. 5b), and a more even distribution of all the different phases. Common to all spectra, however, is a low amount of the original spinel phase. The variance in the relative amounts of the different phases, given in percent (%) in Figure 5, were

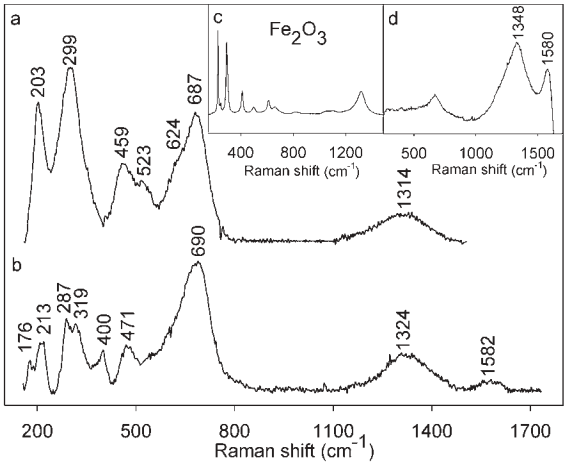

FIGURE 4. Raman spectra (**a**) of mainly the $MgFe_2O_4$ spinel phase, (**b**) of $MgFe_2O_4$ spinel phase and Fe_2O_3, (**c**) of pure Fe_2O_3 for comparison (**d**) of the two strongest peaks with wave numbers >1300 cm^{-1}, possibly microcrystalline graphite.

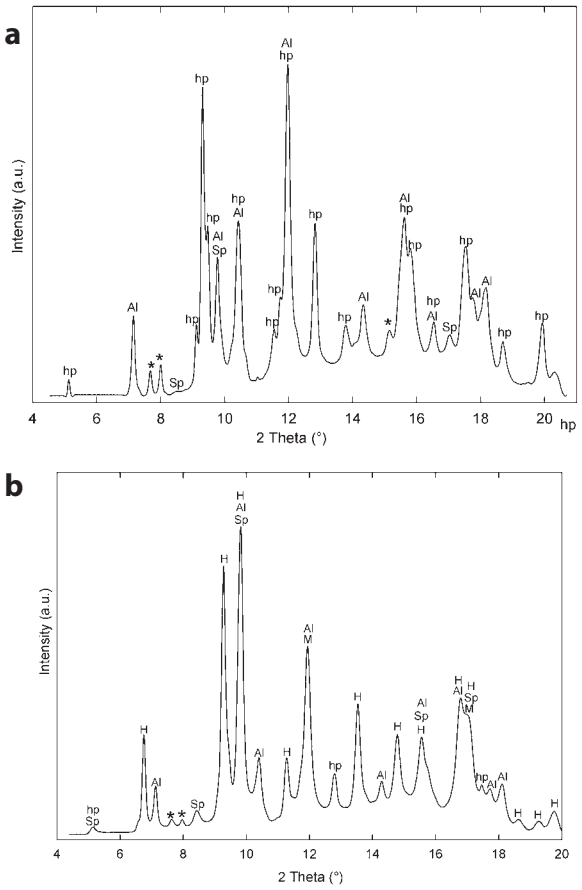

FIGURE 5. (**a**) X-ray diffraction pattern of a mixture of ~1% $MgFe_2O_4$ (Sp), ~39% high-pressure phase (hp), and ~60% Al_2O_3 (Al). Three unidentified peaks are marked with *. (**b**) X-ray diffraction pattern of a mixture of ~24% Fe_2O_3 (H), ~24% MgO (M), ~3% $MgFe_2O_4$ (Sp), ~4% high-pressure phase (hp) and ~45% Al_2O_3 (Al). Two unidentified peaks are marked with *. For clarity reasons weak peaks, overlapped by much stronger peaks, are not marked in the two spectra.

estimated by use of the crystallographic program CaRine, and are due to the temperature gradient in the sample. The peaks in the spectra were indexed from their positions due to a possible preferred orientation and the fact that several peaks of the different phases show overlap. This also makes it difficult to perform a Rietveld analysis.

The high-pressure phase can be indexed by the $CaMn_2O_4$-type structure, space group *Pbcm*, as suggested by Andrault and Bolfan-Casanova (2001). The cell parameters for the high-pressure phase in Figure 5a, calculated with the program Unitcell, are a = 2.775(2), b = 9.283(16), and c = 9.446(5) Å. This gives a unit cell volume of 243.4(4) $Å^3$. The uncertainties shown in parentheses represent standard deviations of the fit. Due to overlap of other phases, not all observed high-pressure peaks were used in the cell parameter calculation. Observed and calculated d-values, used for calculation of the cell parameters in Unitcell (marked with *), are presented in Table 2. For comparison with the results of Andrault and Bolfan-Casanova (2001) we have used our observed cell volume, which corresponds to the pressure 25.7 GPa using their equation of state for the high-pressure phase, to calculate a spectrum at this pressure in CaRine. The calculated d-values are shown in Table 2 and are in good agreement with our observed d-values.

The presence of Fe_2O_3 is clearly seen in the spectrum in Figure 5b, but due to very few diffraction lines and overlap by peaks from other phases, the presence of MgO is difficult to confirm. The cell parameters for Fe_2O_3 in this spectrum are a = 4.937(3) and b = 13.195(13) Å, giving a cell volume of 278.5(3) $Å^3$. Observed and calculated d-values for Fe_2O_3 are presented in Table 3. All d-values were used for cell parameter calculation even though there is some degree of overlap that influences some of the peak positions. Additionally, in Table 3 there is a calculated spectrum for Fe_2O_3. This was made by using our observed cell volume, which corresponds to a pressure of 24.5 GPa, by using the equation of state for Fe_2O_3 given in Rozenberg et al. (2002).

In every spectrum there are also two small, but well resolved, unidentified peaks in the d-ranges 3.15–3.179 and 3.031–3.052 Å; in most of the spectra there is also a third small unidentified peak in the d-range 1.601–1.613 Å (Figs. 5a and 5b).

TABLE 2. Observed d-values (d_{obs}) at 23 ± 2 GPa, calculated d-values in Unitcel1 ($d_{calc, U}$), and calculated d-values at 25.7 GPa in CaRine ($d_{calc, Ca}$) for the high-pressure phase in Figure 5a

hkl	d_{obs} (Å)	$d_{calc, U}$ (Å)	$d_{calc, Ca}$ (Å)
0 0 2*	4.726	4.723	4.703
1 1 0*	2.660	2.659	2.663
0 2 3*	2.605	2.606	2.601
1 1 1*	2.562	2.560	2.563
0 4 0	2.325		2.328
0 2 4*	2.104	2.104	2.099
1 3 0*	2.069	2.069	2.071
1 1 3*	2.027	2.027	2.030
1 3 2*	1.893	1.893	1.895
1 1 4*	1.761	1.761	1.763
1 5 1	1.534		1.527
1 5 2	1.470		1.470
0 6 3*	1.388	1.388	1.391
0 4 6*	1.301	1.301	1.300
2 2 3*	1.222	1.222	1.226

* *hkl* values used for cell parameter calculations.

TABLE 3. Observed *d*-values (d_{obs}) at 23 ± 2 GPa, calculated *d*-values in Unitcell ($d_{calc, U}$) and calculated *d*-values at 24.5 GPa in CaRine ($d_{calc, Ca}$) for the Fe_2O_3 phase in Figure 5b

hkl	d_{obs} (Å)	$d_{calc, U}$ (Å)	$d_{calc, Ca}$ (Å)
0 1 2	3.588	3.588	3.597
1 0 4	2.612	2.612	2.624
1 1 0	2.471	2.468	2.470
1 1 3	2.152	2.152	2.157
0 2 4	1.794	1.794	1.799
1 1 6	1.643	1.642	1.649
2 1 4	1.449	1.451	1.454
3 0 0	1.426	1.425	1.426
2 0 8	1.302	1.306	1.312
1 0 10	1.264	1.261	1.269
2 2 0	1.232	1.234	1.235

DISCUSSION

Theoretically, the breakdown of spinels is possible if the bulk densities of the constituent oxides are higher than for the corresponding spinel structure, which is the case for $MgFe_2O_4$. The increase in density with pressure is due mainly to the increase in coordination number in the oxide mixture. However, instead of the predicted formation of Fe_2O_3 and MgO at increasing pressure, only a direct transformation of the spinel into its high-pressure phase has been observed until now. Since the formation of the breakdown products is predominantly a diffusion-controlled reaction, a displacive rearrangement of the spinel lattice into the high-pressure phase seems to be more favorable when the temperature is too low for diffusion to occur. This is obvious in the case of Fe_3O_4, which is predicted to break down into FeO and Fe_2O_3. The stability field for co-existence of these oxides decreases as temperature increases, with a maximum temperature of 850 K (Lazor et al. 2004, Fig. 3). This rather low temperature makes the kinetics slow and the result is a direct displacive transformation of Fe_3O_4 into its high-pressure polymorph. However, Lazor et al. (2004) did observe weak XRD peaks of Fe_2O_3 in their high-pressure study of Fe_3O_4. These findings are further supported in an upcoming high-pressure study of Fe_3O_4 using Raman spectroscopy (O.N Shebanova and P. Lazor, personal communication). The maximum temperature for the co-existence of the assemblage MgO and Fe_2O_3 is about 950 K higher than for the assemblage FeO and Fe_2O_3 from Fe_3O_4. This is probably the explanation for the formation of breakdown products in our experiments. The failure to experimentally demonstrate the breakdown reaction in earlier studies of $MgFe_2O_4$ is probably also due to slow kinetics. Levy et al. (2004) performed separate high-pressure and high-temperature experiments and did not observe any sign of transformation of their sample up to 35 GPa. Wang et al. (2002) performed their Raman experiments at room temperature and only noticed the transformation to the high-pressure phase, which occurred at ~27 GPa. The reported annealing temperature in Andrault and Bolfan-Casanova (2001), 2500 K, is above the temperature for the stable co-existence of MgO and Fe_2O_3. Mao and Bell (1974) heated their sample at 1500 °C, which is within the region for the breakdown products. However, the short heating time, 15 minutes, was apparently not sufficient for the breakdown reaction to occur. The results of Ringwood and Reid (1969) were inconclusive because a partial reduction of Fe^{3+} to Fe^{2+} took place during the experiments.

The methods we used to study the high-pressure transformations of $MgFe_2O_4$ in DAC, i.e., Mössbauer and Raman spectroscopy and synchrotron XRD, all suggest a multi-phase sample with spinel, breakdown products, and a high-pressure phase.

The in situ Mössbauer investigation illustrates the displacive nature of the high-pressure transformation. The first observation of the high-pressure phase clearly shows a disordered element distribution with Fe^{3+} at two non-equivalent crystallographic positions. The smaller strongly distorted site (site 3 in Fig. 2) is characterized by a low co-ordination number, possibly four, while the second pattern (site 4 in Fig. 2) shows a smaller quadrupole splitting and a larger isomer shift, indicative of a rather regular six coordinated polyhedron. The initial "inversion parameter" for the high-pressure phase is about the same as for the original spinel structure. But with increasing pressure and successive heating, iron diffuses from site 3 into site 4. At the same time, the coordination number of site 3 increases, as shown by a rapid increase in isomer shift (Fig. 3), probably toward eight as in the ideal ordered $CaMn_2O_4$-type structure. After decompression of the second DAC, the high-pressure phase is dominated by one doublet in the Mössbauer spectra. This indicates that Fe now occupies the octahedral sites and Mg the dodecahedral site. The observed slow kinetics of the high-pressure transformation over a wide range of pressures is suggested to be the result of inhomogeneous strain in the sample chamber at high pressure and a competition between the reactions forming breakdown products and a high-pressure phase. The two alternative fits of the small doublet in the decompressed spectrum give two different possible results. An IS of 0.63 mm/s for this pattern could indicate a still-existing site 3. This higher value, compared to an IS of 0.45 mm/s at 29 ± 4 GPa, would then be explained by a decrease in electron density at the nucleus due to decompression. An IS of 0.9 mm/s for that doublet is too high to come from Fe^{3+} and suggests formation of a $(Mg,Fe^{2+})O$ solid solution, indicating somewhat reducing conditions in the DAC during the experiments. If this is the case the $(Mg, Fe^{2+})O$ doublet should also be present in the high-pressure spectrum at 29 ± 4 GPa. Fitting of an additional $(Mg, Fe^{2+})O$ pattern in Figure 2c is possible without any dramatic change of the parameters for the other sites. The composition of the $(Mg,Fe^{2+})O$ solid-solution would be close to the MgO-end member as shown by the large quadropole splitting (McCammon 1995). The presence of Fe_2O_3 and a possible presence of $(Mg, Fe^{2+})O$ seen in the Mössbauer spectrum after decompression demonstrates the partial breakdown of the $MgFe_2O_4$ sample.

Although the hyperfine parameters differ for the high-pressure phase between the two DAC values in the Mössbauer experiments, both show the same features with two paramagnetic doublets that change intensities and hyperfine parameters with increasing pressure. The discrepancy, seen as a lower IS and QS in DAC 2 compared to DAC 1, could be explained by a smaller pressure gradient in DAC 2. A direct pressure increase in DAC 2, to 24 ± 4 GPa, instead of a stepwise increase as in DAC 1, may also be a contributing factor to the differences. The higher counting rate during Mössbauer measurements on DAC 2 also gives better-resolved spectra and makes the fitting procedure more straightforward. No spectrum was obtained from DAC 1 after the pressure was released; this makes it difficult to confirm if Fe_2O_3 was also present in this DAC. However, the lower mag-

netic fields measured for the sextets in DAC 1 do not indicate the presence of Fe_2O_3. The explanation for this may also lie in the stepwise vs. direct pressure increase in the two DACs. The presence of Fe_2O_3 in the decompressed sample, DAC 2, is further supported by Raman spectroscopy. However, there is only one Fe_2O_3 peak at 400 cm^{-1} that is not affected by overlap from other phases. Besides having $MgFe_2O_4$ and Fe_2O_3 in the sample, we also suggested the possible presence of carbon phases. This assumption is based mainly on the spectrum in Figure 4d, which is very similar to some of the spectra published in Prakapenka et al. (2003/2004). The possible presence of carbon in our sample would then affect and overlap any Fe_2O_3 peaks at Raman shifts > 1300 cm^{-1}. However, based on the intensity ratio of the two peaks in our spectra, we believe that the main contribution comes from Fe_2O_3 rather than from carbon phases.

The origin of the unidentified peaks, which occur in every XRD spectrum, remains unresolved. One tempting explanation is the possibility of a reaction between Al_2O_3 and MgO, after breakdown of $MgFe_2O_4$, forming the high-pressure phase of $MgAl_2O_4$ (Irifune et al. 1991; Funamori et al. 1998). Alternatively, a reaction between Al_2O_3 and $MgFe_2O_4$ could possibly result in a solid-solution, as a spinel or the high-pressure modification of the spinel. However, these reactions cannot fully explain the present observations because they require the presence of Fe_2O_3. Fe_2O_3 is absent in some of the XRD spectra, while the unidentified peaks are always present.

The concurrent presence of spinel, a high-pressure phase, and breakdown products implies annealing temperatures both below and above the critical temperature around 1800 K, as shown in Figure 1 (Levy et al. 2004). Thus, two reactions occur at high pressure using laser annealing:

$$\text{At } T < 1800 \text{ K: } MgFe_2O_4 \rightarrow Fe_2O_3 + MgO \quad (1)$$

$$\text{At } T > 1800 \text{ K: } MgFe_2O_4 \rightarrow \text{hp-}MgFe_2O_4 \quad (2)$$

The difference in annealing temperature is also obvious when comparing the two-dimensional XRD images in Figures 6a and b. Figure 6a is a spectrum dominated by the breakdown products Fe_2O_3 and MgO. The fact that this spot has been exposed to a lower heating temperature, resulting in breakdown, is seen by the continuous diffraction lines. Figure 6b, on the other hand, shows spotty diffraction lines coming from large crystal particles caused by the growth of the high-pressure phase of $MgFe_2O_4$, enhanced by a higher temperature.

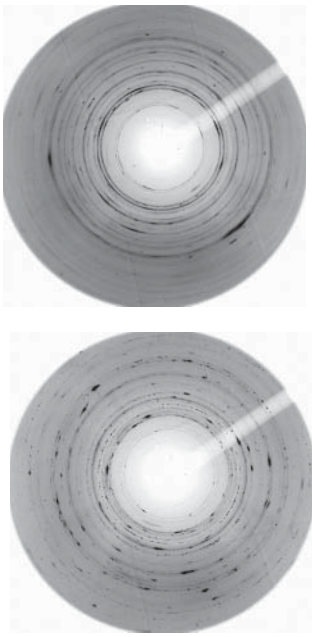

FIGURE 6. Two-dimensional XRD images of (**a**) a spectrum exposed to lower heating temperature, resulting in formation of the breakdown products Fe_2O_3 and MgO and (**b**) a spectrum exposed to a higher heating temperature resulting in crystal growth of the high-pressure phase of $MgFe_2O_4$.

ACKNOWLEDGMENTS

We thank P. Lazor for valuable discussions and scientific assistance and S. Sundberg for assistance with the Raman spectroscopy. The XRD measurements benefited from discussions with G. Shen. We thank Ö. Amcoff for critical reading of the manuscript. Valuable comments from the referees, which improved our manuscript, are acknowledged.

REFERENCES CITED

Andrault, D. and Bolfan-Casanova, N. (2001) High-pressure phase transformations in the $MgFe_2O_4$ and Fe_2O_3-$MgSiO_3$ systems. Physics and Chemistry of Minerals, 28, 211–217.

d'Amour, H., Schiferl, D., Denner, W., Schulz, H., and Holzapfel, W.B. (1978) High-pressure single-crystal structure determination for ruby up to 90 kbar using an automatic diffractometer. Journal of Applied Physics, 49, 4411–4416.

Dubrovinsky, L.S., Dubrovinskaia, N.A., McCammon, C., Rozenberg, G.Kh., Ahuja, R., Osorio-Guillen, J.M., Dmitriev, V., Weber, H-P., Le Bihan, T., and Johansson, B. (2003) The structure of the metallic high-pressure Fe_3O_4 polymorph: Experimental and theoretical study. Journal of Physics: Condensed Matter, 15, 7697–7706.

Fei, Y., Frost, D.J., Mao, H-K., Prewitt, C.T., and Häusermann, D. (1999) In situ structure determination of the high-pressure phase of Fe_3O_4. American Mineralogist, 84, 203–206.

Funamori, N., Jeanloz, R., Nguyen, J.H., Kavner, A., Caldwell, W.A., Fujino, K., Miyajima, N., Shinmei, T., and Tomioka, N. (1998) High-pressure transformations in $MgAl_2O_4$. Journal of Geophysical Research, 103, 20813–20818.

Greenwood, N.N. and Gibb, T.C. (1971) Mössbauer spectroscopy, 659 p. Chapman and Hall Ltd, London.

Haavik, C., Stølen, S., Fjellvåg, H., Hanfland, M., and Häusermann, D. (2000) Equation of state of magnetite and its high-pressure modification: Thermodynamics of the Fe-O system at high pressure. American Mineralogist, 85, 514–523.

Hammersley, A.P., Svensson, S.O., Hanfland, M., Fitch, A.N., and Häusermann, D. (1996) Two-dimensional detector software: From real detector to idealized image or two-theta scan. High Pressure Research, 14, 235–245.

Huang, E. and Bassett, W.A. (1986) Rapid determination of Fe_3O_4 phase diagram by synchrotron radiation. Journal of Geophysical Research, 91, 4697–4703.

Irifune, T., Fujino, K., and Ohtani, E. (1991) A new high-pressure form of $MgAl_2O_4$. Nature, 349, 409–411.

Jernberg, P. and Sundqvist, T. (1983) A versatile Mössbauer analysis program. Institute of Physics, University of Uppsala, report UUIP-1090.

Lazor, P., Shebanova, O.N., and Annersten, H. (2004) High-pressure study of stability of magnetite by thermodynamic analysis and synchrotron X-ray diffraction. Journal of Geophysical Research, 109, B05201.

Levy, D., Diella, V., Dapiaggi, M., Sani, A., Gemmi, M., and Pavese, A. (2004) Equation of state, structural behaviour and phase diagram of synthetic $MgFe_2O_4$, as a function of pressure and temperature. Physics and Chemistry of Minerals, 31, 122–129.

Liu, L-g. (1975) Disproportionation of $MgAl_2O_4$ spinel at high pressures and temperatures. Geophysical Research Letters, 2, 9–11.

Mao, H.K. and Bell, P.M. (1974) High-pressure transformation in magnesioferrite ($MgFe_2O_4$). Carnegie Institution of Washington YearBook, 75, 555–557.

Mao, H-K., Takahashi, T., Bassett, W.A., Kinsland, G.L., and Merrill, L. (1974) Isothermal compression of magnetite to 320 kbar and pressure-induced phase transformation. Journal of Geophysical Research, 79, 1165–1170.

Mao, H.K., Virgo, D., and Bell, P.M. (1977) High-pressure ^{57}Fe Mössbauer data on the phase and magnetic transitions of magnesioferrite ($MgFe_2O_4$), magnetite

(Fe_3O_4), and hematite (Fe_2O_3). Carnegie Institution of Washington YearBook, 76, 522–525

Massey, M.J., Baier, U., Merlin, R., and Weber, W.H. (1990) Effects of pressure and isotopic substitution on the Raman spectrum of α-Fe_2O_3: Identification of two-magon scattering. Physical Review B, 41, 7822–7827.

McCammon, C. (1995) Mössbauer spectroscopy of minerals. In T.J. Ahrens, Ed., A Handbook of Physical Constants, 2, 400. American Geophysical Union, Washington, D.C.

McCarty, K.F. (1988) Inelastic light scattering in α-Fe_2O_3: Phonon vs. magnon scattering. Solid State Communications, 68, 799–802.

O'Neill, H.St.C, Annersten, H., and Virgo, D. (1992) The temperature dependence of the cation distribution in magnesioferrite ($MgFe_2O_4$) from powder XRD structural refinements and Mössbauer spectroscopy. American Mineralogist, 77, 725–740.

Pasternak, M.P., Nasu, S., Wada, K., and Endo, S. (1994) High-pressure phase of magnetite. Physical Review B, 50, 6446–6449.

Prakapenka, V.B., Shen, G., and Dubrovinsky, L.S. (2003/2004) Carbon transport in diamond anvil cells. High Temperatures-High Pressures, 35/36, 237–249.

Ringwood, A.E. and Reid, A.F. (1969) High pressure transformations of spinels (I). Earth and Planetary Science Letters, 5, 245–250.

Rozenberg, G.Kh., Dubrovinsky, L.S., Pasternak, M.P., Naaman, O., LeBihan, T., and Ahuja, R. (2002) High-pressure structural studies of hematite Fe_2O_3. Physical Review B, 65, 064112.

Shim, S-H. and Duffy, T.S. (2002) Raman spectroscopy of Fe_2O_3 to 62 GPa. American Mineralogist, 87, 318–326.

Wang, Z., Lazor, P., Saxena, S.K., and O'Neill, H.St.C. (2002) High pressure Raman spectroscopy of ferrite $MgFe_2O_4$. Materials Research Bulletin, 37, 1589–1602.

MANUSCRIPT RECEIVED MARCH 22, 2005
MANUSCRIPT ACCEPTED JULY 9, 2005
MANUSCRIPT HANDLED BY DARBY DYAR